Reports of Practical Oncology and Radiotherapy 25 (2020) 470–478

Available online at www.sciencedirect.com

Reports of Practical Oncology and Radiotherapy

journal homepage: http://www.elsevier.com/locate/rpor

Original research article

Monte carlo model and output factors of elekta infinity™ 6 and 10 MV photon beam

Sitti Yani [a,b,⁎], Indra Budiansah [b], Mohamad Fahdillah Rhani [c], Freddy Haryanto [b]

[a] Department of Physics, Faculty of Mathematics and Natural Sciences, IPB University (Bogor Agricultural University), Babakan, Bogor, Indonesia
[b] Department of Physics, Faculty of Mathematics and Natural Sciences, Institut Teknologi Bandung, Jalan Ganesa 10, Bandung, Indonesia
[c] Radiology Department, Concord International Hospital, 19 Adam Road, Singapore, Singapore

ARTICLE INFO

Article history:
Received 19 July 2019
Received in revised form 2 February 2020
Accepted 20 March 2020
Available online 28 April 2020

Keywords:
Commissioning
Elekta infinity™
Photon beam
Output factors

ABSTRACT

Aim: This study aimed to commission the Elekta Infinity™ working in 6 and 10 MV photon beam installed in Concord International Hospital, Singapore, and compare the OFs between MC simulation and measurement using PTW semiflex and microDiamond detector for small field sizes.
Material and Methods: There are two main steps in this study: modelling of Linac 6 and 10 MV photon beam and analysis of the output factors for field size 2×2–$10 \times 10\,cm^2$. The EGSnrc/BEAMnrc-DOSXYZnrc code was used to model and characterize the Linac and to calculate the dose distributions in a water phantom. The dose distribution and OFs were compared to the measurement data in the same condition.
Results: The commissioning process was only conducted for a $10 \times 10\,cm^2$ field size. The PDD obtained from MC simulation showed a good agreement with the measurement. The local dose difference of PDDs was less than 2% for 6 and 10 MV. The initial electron energy was 5.2 and 9.4 MeV for 6 and 10 MV photon beam, respectively. This Linac model can be used for dose calculation in other situations and different field sizes because this Linac has been commissioned and validated using Monte Carlo simulation. The 10 MV Linac produces higher electron contamination than that of 6 MV.
Conclusions: The Linac model in this study was acceptable. The most important result in this work comes from OFs resulted from MC calculation. This value was more significant than the OFs from measurement using semiflex and microDiamond for all beam energy and field sizes because of the CPE phenomenon.

1. Introduction

Monte Carlo (MC) simulation is considered as the most accurate method of radiation dose calculation in radiotherapy and has become a common method for benchmarking the other dose calculation methods in homogenous and inhomogeneous cases. Some MC codes are widely used in medical physics including EGSnrc,[1–8] MCSP,[9] MCNP,[10–12] Penelope,[13,14] Geant4,[15,16] and XVMC.[17] Each code has different advantages and disadvantages related to the simulation time and output of physical factors obtained at the end of the simulation. Simulation studies were a critical aspect to understand the physical factors when experimental measurements are not feasible.

Development of an MC beam model for linear accelerators (Linacs) is the first and most crucial step in Monte Carlo dose calculations in phantoms or humans. Dose calculation error can occur due to errors in material and geometry selection when building Linac. Many studies have been conducted relating to modelling Linac and characterize the Linac output.[18–22] Some studies matched the calculated and measured percent depth dose (PDD) curves for tuning electron beam energy. Haryanto et al. found that profiles and depth dose distributions resulting from the simulation have a good agreement with the measurements in 2×2 and $10 \times 10\,cm^2$ field sizes.[18] An Elekta Sl*i* plus 6 MV photon beam was modeled using EGSnrc. Varian Trilogy (2300C/D) linear accelerator was build using BEAMnrc by Borges et al.[19] The dose discrepancies for dose profiles, with and without 120 leaves HD MLC, between the measurements and the opened field simulations using ionization chambers in a water phantom, were less than 5%. Toutaoui et al. (2014) used the EGSnrc MC code to model Siemens Primus 6 MV photon beam Linac. The dose distribution was calculated in various phantoms. The results show that there is a good agreement between MC simulation and measurement in a water phantom.[20] In our previous study, the Varian Trilogy Clinac iX 6 and 10 MV photon beam installed in Tan Tock Seng Hospital, Singapore, was conducted. We found that the initial electron energy chosen to simulate this Linac was 6.4 and

* Corresponding author.
E-mail addresses: sittiyani@apps.ipb.ac.id, sitti.yani@gmail.com (S. Yani).

https://doi.org/10.1016/j.rpor.2020.03.021
1507-1367/

10.3 MeV for 6 and 10 MV, respectively. The local dose difference of PDD and profile dose with measurement data was less than 5%[6,7] The output factors in a small field size have been evaluated in this study.

Charged particle equilibrium and high dose gradient were absent in the small field. The various detectors used in dose distribution measurement were limited. Several researchers measured and calculated the output factors (OFs) using different detectors and Monte Carlo simulation.[23–25] Haryanto et al. (2004), Das et al. (2008), Fan et al. (2009), and Bassinet et al. (2013) reported that OFs of small photon fields measured with different detectors can vary up to 30%, and, clearly, such differences are not acceptable in radiation therapy.[18,26–28]

The total scatter photon of the three collimators (diameter 5–10 mm) of the Cyberknife radiosurgery was measured in experimental measurement and Monte Carlo simulation. This study was conducted by Francescon et al. (2008). They collected the experimental data using two microchambers, a diode, and a diamond detector. The total scatter photon varied with the spatial distribution of the electron beam with the uncertainty of less than 2%.[29]

Cheng et al. (2016) measured the OFs for Varian TrueBeam 6 and 10 MV flattening filter-free photon beam in a stereotactic radiosurgery system. In this research, they used two small diode detectors Edge (Sun Nuclear) and Small Field Detector (SFD) (IBA Dosimetry) to determine the OFs in measurement. The deviation of OFs between measurement and MC simulation was less than 3% for conical collimator diameter $\geq$ 12.5 mm. For conical diameter less than 12.5 mm, the deviation between measurement and MC had a more considerable variation.[30]

Krongkietlearts et al. (2016) found that the percentage difference of relative OFs from measurement (microDiamond and semiflex detector) and MC simulation in Varian Clinac iX6 MV photon beam was less than 2%. The OFs were measured in 5 and 10 cm for field size 1×1–5×5 cm^2.[31]

Godson et al. (2016) studied the small field OFs of BrainLab circular cones, BrainLab mMLC, and Millennium MLC. They found the differences of OFs between all different detectors for all collimating systems. The detectors orientation (parallel and perpendicular orientation to the central axis) and the position of the collimator could have a considerable influence on the output factors in small fields.[32]

1.1. Aim

Each Linac modeled using Monte Carlo code has different characteristics, which results in different PDD, dose profile, and OFs obtained. Several simulation parameters, such as voxel sizes, range rejection methods, and particles cut-off energy affect the outputs at the end of the simulation. Therefore, this study aimed to commission the Elekta Infinity™ working in 6 and 10 MV photon beam installed at the Concord International Hospital, Singapore, and compare the OFs between MC simulation and measurement using PTW semiflex and microDiamond detector for small field sizes. The EGSnrc/BEAMnrc-DOSXYZnrc code was used to model and characterize the Linac and to calculate the dose distributions in a water phantom. The dose distribution and OFs were compared to the measurement data in the same condition and set up. Research on the EGSnrc modelling of 10 MV photon beam from the Elekta Infinity™ is quite innovative. Study of Elekta Infinity 6 MV photon beam using EGSnrc/BEAMnrc has been done previously by Gholampourkashi et al. (2018).[33] However, the method of determining the initial electron energy and full width at half maximum (FWHM) in the commissioning process was very different from the method used in this study.

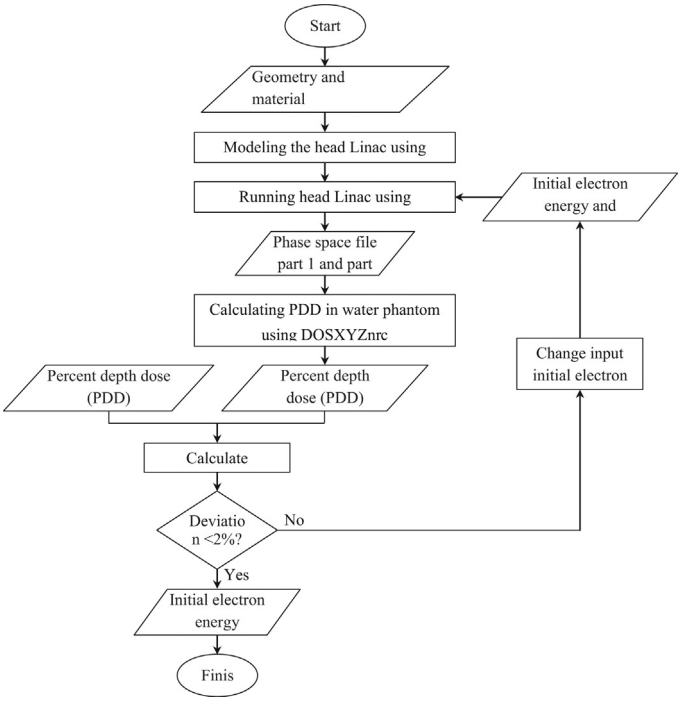

Fig. 1. Flowchart of determination of Linac initial electron energy.

2. Materials and methods

The material and methods utilized for Monte Carlo simulation and measurements to calculate dose distribution and output factors were presented in this section.

2.1. Monte Carlo user code

In the present work, all MC simulations were performed using EGSnrc Monte Carlo user codes – a Monte Carlo simulation package of coupled photon-electron transport in geometry with energy ranges from 1 keV to several hundreds of GeV. This code, including BEAMnrc and DOSXYZnrc user code,[34,35] was used to model the Elekta Infinity linear accelerator with mlc and calculate dose distributions in the water phantom, respectively. The measurements and Monte Carlo simulations were performed on a medical accelerator Elekta Infinity™ operating at 6 and 10 MV photon beam installed at the Radiotherapy Department, Concord International Hospital, Singapore.

2.2. Simulation of interactions in Elekta Infinity treatment head

The commissioning process was carried out in two phases, namely energy beam and Linac geometry commissioning. The steps were described in Fig. 1 and 2. These phases aim to determine the initial electron beam for each beam (6 and 10 MV) and geometry of Linac (mlc opening to adjust the specific field size).

The energy beam commissioning steps carried out in this study are shown in Fig. 1. The steps include modelling Linac 6 and 10 MV, running the Linac modeled with varied initial electron energy and fixed full width at half maximum (FWHM), calculating dose distribution in a water phantom, and calculating the PDD deviation between Monte Carlo simulation and measurement. The FWHM refers to the Gaussian distribution of the beam in the Z-direction. Simulations were run in parallel on a four core Linux operating system. Some parameters applied in the Monte Carlo simulation are as follows:

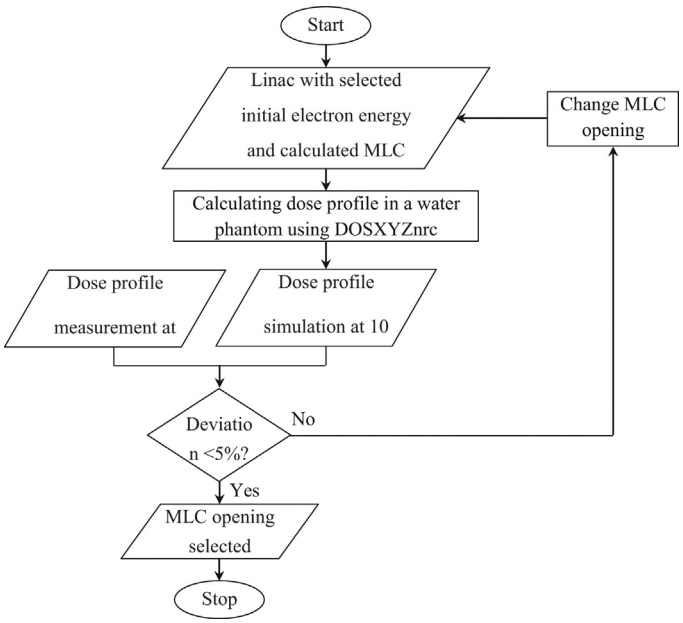

Fig. 2. Flowchart of beam geometry determination.

The cut-off energy for electron transport (ECUT) and photon transport (PCUT) were set at 0.7 MeV and 0.01 MeV, respectively

The variance reduction techniques, such as Bremsstrahlung splitting, Russian Roulette, Range Rejection, and Photon Forcing were not applied.

a) Modeling of head Linac

All beams were provided by an Elekta Infinity™ linear accelerator equipped with an Elekta MLC Infinity multileaf collimator that consists of 80 pairs of tungsten leaves as a tertiary collimating system. The maximum adjustable field size was $40 \times 40\,cm^2$. The material composition of mlc leaf is 95% tungsten, 3.75% nickel, and 1.25% iron with density of $18\,g/cm^3$ (Elekta AB, Stockholm, Sweden).

A schematic representation of the Linac head and its components is shown in Fig. 3. The linac head components, including the target, primary collimator, different filter, flattening filter, mirror, multileaf collimator, and JAWS, were simulated based on manufacturer-provided information. All the components were common for 6 and 10 MV, except for different filter. The different filter is only utilized by high energy Linac (10 MV). The component modules used in BEAMnrc for 6 and 10 MV photon beam modelling different sections of the Linac head were SLABS for the target, FLATFLIT for the primary collimator, different filter, and flattening filter, CHAMBER for the monitor chamber, MIRROR for the mirror, MLCE for multileaf collimator (mlc), JAWS for the JAWS, and SLABS for the air gap between JAWS and phantom. The scoring planes were placed above mlc (Linac part 1) and in the source to surface distance (SSD) of 100 cm from the target (Linac part 2). The field size arrangement is made by arranging the mlc leafs opening.

b) Running head Linac

A monoenergetic electron beam was defined above the tungsten target. Photon bremsstrahlung can be produced from the interaction between the electron beams that hit the target. Photons (bremsstrahlung) were produced from the deceleration of the electron beam in the target. After passing the target, produced photons will have a continuous spectrum with an energy range from zero to electron beam energy. The average energy of this photon is one

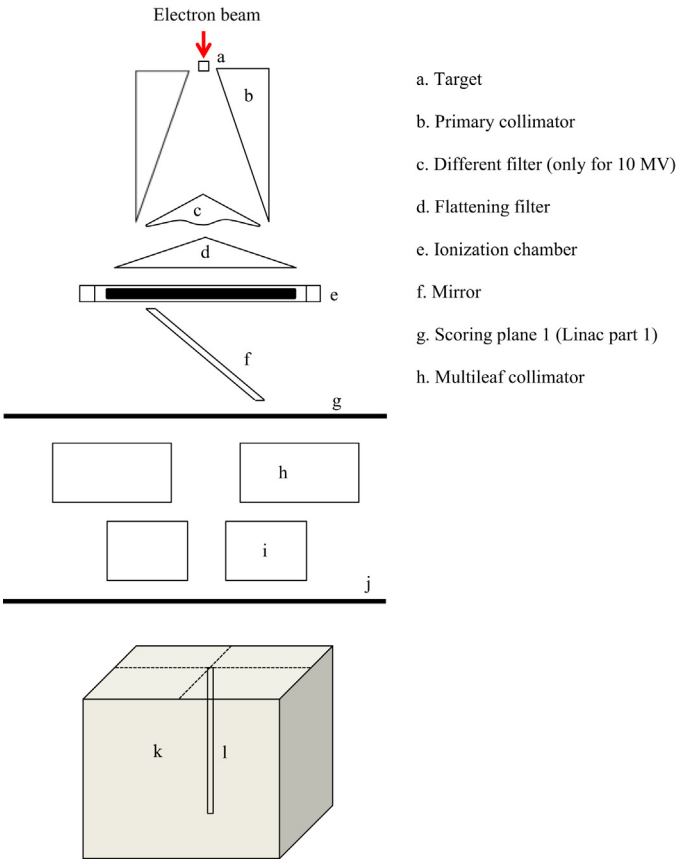

Fig. 3. Sketch of Elekta Infinity™ and water phantom.

third of the maximum electron energy.[36] The spatial photon distribution is converted to more homogeneous shape by using the different filter and flattening filter for use in clinical purposes.

The tuning of the Linac simulation is obtained by varying the initial electron energy and FWHM of the simulation until a match is found between different measured and calculated PDD and dose profiles for field size $10 \times 10\,cm^2$.

At the end of this step, 12 phase space (phsp) files (Linac part 1 = 6 phsp files in scoring plane 1 and Linac part 2 = 6 phsp files in scoring plane 2) for 6 MV and 10 phsp files for 10 MV (Fig. 2). The phsp in scoring plane 1 was used as input to produce the phsp file in scoring plane 2 with fixed field size in BEAMnrc and, subsequently, the second phsp file was used to produce the dose distribution in a water phantom in DOSXYZnrc. The stored phsp files were used repeatedly as source inputs. These two files were analyzed to obtain information of stored particles in scoring planes such as the number of particles in a phsp file, particles angular distribution, particle fluence, mean energy, and spectral distribution using BEAMDP (BEAM Data Processing). The size of a phase-space file was about 2 GB.

The phsp file contains the following data for each particle crossing the scoring plane:

$$P = [x, y, z, u, v, E, q, weight, LATCH] \quad (1)$$

where x and y are the position coordinates of the particle in specific z (z is scoring plane position); u and v are the direction cosines in the x and y directions, respectively; E is the particle energy; q is the particle charge (0, -1, and +1 for photon, electron, and positron, respectively); weight is the particle statistical weight; and LATCH is a tag that records where particles previously originated or interacted. The phase space plane was perpendicular to the beam axis.[34]

Precise modelling of the 10 MV LINAC gantry and a sufficiently large number of particles are required to obtain accurate results

from Monte Carlo simulations in radiotherapy calculations. In order to achieve similar standard deviations, the number of primary events needed for fields of larger size is smaller than that for narrow fields: 2×10^{10} primary electrons for a $2 \times 2\,cm^2$ field, 1.2×10^{10} electrons for a $3 \times 3\ cm^2$ field, 5.7×10^9 primary electrons for a $5 \times 5\,cm^2$ field, 3×10^9 primary electrons for a $6 \times 6\ cm^2$ field, 1.8×10^9 primary electrons for a $8 \times 8\,cm^2$ field and 5×10^8 primary electrons for a $10 \times 10\,cm^2$ field. The simulation time to produce a phsp file in scoring plane 2 depends on the field width, the number of particles simulated, and Linac energy.

c) Calculation of dose distributions in a water phantom

The $40 \times 40 \times 40\,cm^3$ simulated water phantom was divided into $38 \times 3 \times 3$ voxels for $10 \times 10\,cm^2$ field size and SSD 100 cm. The voxel size was ranged in volume from 0.2 to $0.5\,cm^3$ depending on the voxel position (surface, build-up, or tail region) for 10 MV PDD calculation. These divisions were not equal in size to minimize the total number of voxels while maintaining excellent resolution and short simulation time where needed. In the penumbral region of the profiles the width of the voxels was 0.2 cm. PDD curves were calculated in the $0.2 \times 0.2 \times 0.2\,cm^3$ voxel around the surface and build-up region. The dose profiles were calculated at a depth of 10 cm for the insensity to the effect of contamination electrons for field size $10 \times 10\,cm^2$ and SDD 100 cm. The number of voxels for dose profile calculation was $61 \times 3 \times 3\ cm^3$ with the voxel size in the x-direction ranged from 0.2 to 1.0 cm. The $0.2 \times 0.2 \times 0.2\,cm^3$ voxel was in the penumbra region (the region with dose 20-80%). In the central beam axis, the voxel dimension was more significant than in the penumbra region. The statistical uncertainties of the simulated dose values were generally less than 1%.

All measurements for percent depth dose (PDD) and dose profiles were made using PTW semiflex 3D 0.07 cc, water equivalent detector, with an active volume of $3.8\,mm^3$ (31021, PTW, Freiburg Germany), mounted on an MP3 scanning system (PTW, Freiburg Germany). The build-up cap was removed during measurement. The uncertainty of the position accuracy of the scanning system provided by the manufacturer was ±0.1 mm. The inner dimensions of the water tank were $40 \times 40 \times 40\,cm^3$. The detector was moved in the water phantom along the z-axis in the center beam axis from the bottom to the water surface in the PDD measurement. Dose profiles are measured along the x- and y-direction perpendicular to the central beam axis. The non-CT image data was used in DOSXYZnrc simulation.

d) Calculate deviation between measurement and MC calculation

PDDs and beam profiles for $10 \times 10\,cm^2$ field size were calculated and compared with measured data. The dosimetric performance of the MC simulation was evaluated against measurement by calculating the deviation (d) between calculated dose from measurement (D_{calc}) and MC simulated dose (D_{MC}) expressed as a percentage of the local dose difference for each point as the following equation.

$$Local\ dose\ difference\ (\%) = \frac{D_{MC} - D_{calc}}{D_{calc}} \times 100\% \quad (2)$$

A cube interpolation was carried out for PDD and dose profile data from MC calculation to equalize data points before calculating local dose difference. The measurement data and Monte Carlo calculation for PDD ranged from 0 to 39 cm with increment of 0.2 to 0.5 cm and 0–31 cm with increment of 0.1 cm, respectively.

Geometry commissioning (mlc opening) was done in Fig. 2. The dose profile in 10 cm depth was calculated using MC simulation and compared with measurement in the same depth. This mlc opening will be chosen as standard to simulate the $10 \times 10\,cm^2$ field size if the deviation between calculation and measurement is less than 5% in the selected region (tail, penumbra, and central beam axis). Eq. (2) was used to calculate the deviation stated as the percentage of local dose difference.

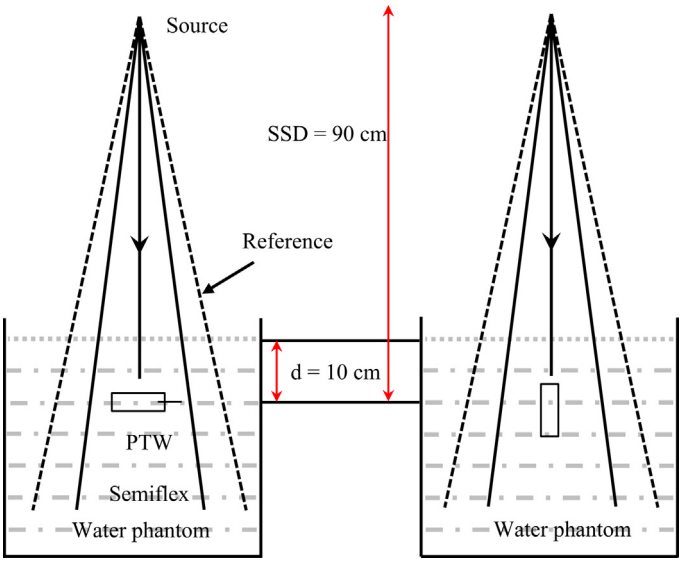

Fig. 4. Geometric arrangement for the OF measurement in a water phantom at a fixed depth and for the reference field sizes.

2.3. Output factor measurement

The photon output factors (OFs) of high-energy Linac describe the relative dose variation of reference field size to another field sizes. OF is defined as the ratio of dose in water D_w for a given field size A at a reference depth d and SSD to the dose at the same depth d and SSD for the reference field size A_{ref}:

$$OFs\,(A) = \frac{Dose\ (A;\ d;\ SSD)}{Dose\ \left(A_{ref};\ d;\ SSD\right)} \quad (3)$$

The depth and SSD used in this study were set to 10 cm and 100 cm, respectively, in measurement and MC calculation. The 10 cm depth was chosen to avoid the effect of electron contamination from Linac head in the measurements.

OFs were measured using PTW semiflex 3D 0.07 cc farmer type and microDiamond for square field sizes ranging from 2×2, 3×3, 5×5, 6×6, 8×8 and $10 \times 10\,cm^2$. PTW semiflex 3D type 31021 ionization chamber was used with area density of $0.084\,g/cm^3$, electrode material with diameter of 0.7 cm, electrode material of4.48 cm in length, and an active volume of 0.078 cm^3. The second detector was microDiamond (solid-state detector) with area density $0.1\,g/cm^3$, diameter of active volume 0.069 cm, length of active volume 0.0954 cm, and active volume of 0.019 cm^3. The encapsulation material of PTW semiflex and microDiamond was PMMA + Graphite and RW3+Epoxy + Al + Air, respectively. All the OFs were taken with these detectors in a water phantom in the central beam axis and isocentrically positioned at a certain reference depth. The setup used is SSD 90 cm and dosimeter at 10 cm depth with perpendicular orientation for PTW Semiflex and parallel orientation for microDiamond (Fig. 4). The output factors only scored in one voxel at 10 cm depth, and the dose value was normalized with $10 \times 10\,cm^2$ field size.

The DOSXYZnrc simulation set up for OFs MC calculation was done using the same setting with the measurement. The field of $10 \times 10\,cm^2$ was used as a reference field size for all output factors at an SSD of 100 cm. A water phantom of $40 \times 40 \times 40\,cm^3$ and voxel size of $0.2 \times 0.2 \times 0.2\,cm^3$ were simulated for both energies. The

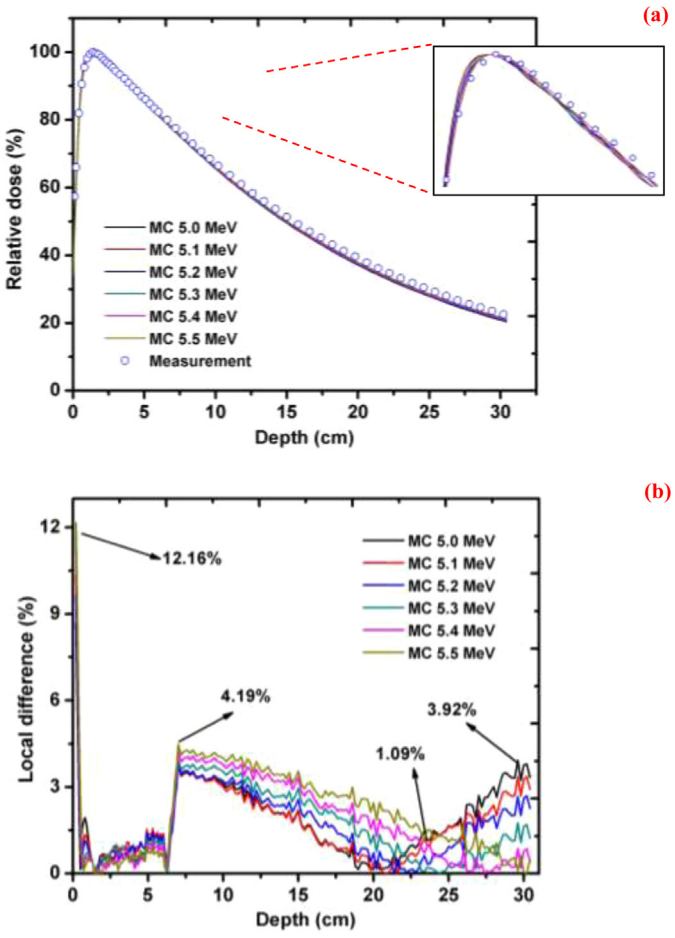

Fig. 5. (a) Calculated and measured PDDs for the 6 MV Elekta Infinity™ photon beam and the (b) local dose difference between measurement and calculation.

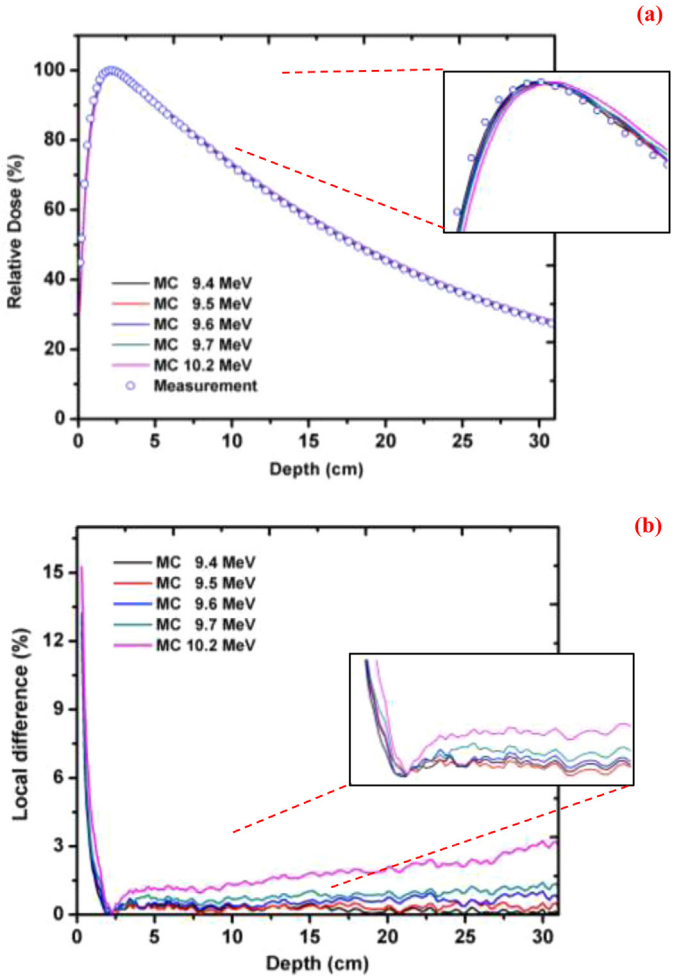

Fig. 6. (a) Calculated and measured PDDs for the 10 MV Elekta Infinity™ photon beam and the (b) local dose difference between measurement and calculation.

same number of incident particle in the phantom surface was used (3×10^8 particles).

OFs deviation between MC calculation and measurement (semi-flex and microDiamond detector) was also calculated using sum root square equation as follows:

$$OFs\ Deviation = abs\left(\frac{OFs\ (calculation) - OFs\ (measurement)}{OFs\ (measurement)}\right) \times 100\% \quad (4)$$

3. Results

In radiation therapy, two important concepts were used for dose distribution of a clinical linear accelerator on the quality control measurements. These concepts are PDD and dose profiles curves. Percentage depth dose curve provides information about the quality of the beam produced by Linac. Dose profile curve indicates the Linac geometry for different field sizes.

3.1. Determination of incident electron energy

By running the phsp file part 2 for PDD calculation in DOSXYZnrc, the statistical uncertainty of the results was less than 1.5% at each point in the water phantom. Comparing the calculated and measured PDD for $10 \times 10\ cm^2$ field size, the mean energy of the electron beam for 6 and 10 MV photon was determined as 0.356 and 0.896 MeV, respectively. Fig. 5 (a) shows a PDD comparison between measurements and MC calculations with varied incident electron energy for 6 MV photon beam. The average of local dose difference between measurement and calculation was 1.87, 1.86, 1.81, 1.86, 1.93, and 2.19 for 5.0, 5.1, 5.2, 5.3, 5.4, and 5.5 MeV, respectively.

All the local differences are less than 5% for the descending part of the curves (Fig. 5(b)). Beyond the dose build-up region (> 1 cm), the measurement and MC simulation data agree closely with the percentage difference of less than 2% for both 6 MV and 10 MV. Increased variation of the dose in build-up area for both energies may be due to limitations in performing accurate measurements, as written in the Report of AAPM Task Group No. 105.[37] The statistical uncertainty of the dose profile in each data point was less than 0.1%. The relative dose was obtained by normalizing the absorbed dose values to a depth of maximum dose for all PDDs curves. For depths near the surface, the local dose difference could be larger than in the build-up or tail region due to the increased uncertainties of both measurements and calculations in the dose build-up area. From these PDD results, we conclude that the best agreement is

obtained for 5.2 MeV.

Fig. 6 shows the PDD comparison between measurement and MC calculation in the same data points for 10 MV photon beam and the local dose difference of each point. Fig. 6 (a) shows a PDD comparison between measurements and MC calculations with varied incident electron energy for 10 MV photon beam. The average of local dose difference between measurement and calculation was 0.72, 0.84, 1.04, 1.29, and 2.22 for 9.4, 9.5, 9.6, 9.7, and 10.2 MeV

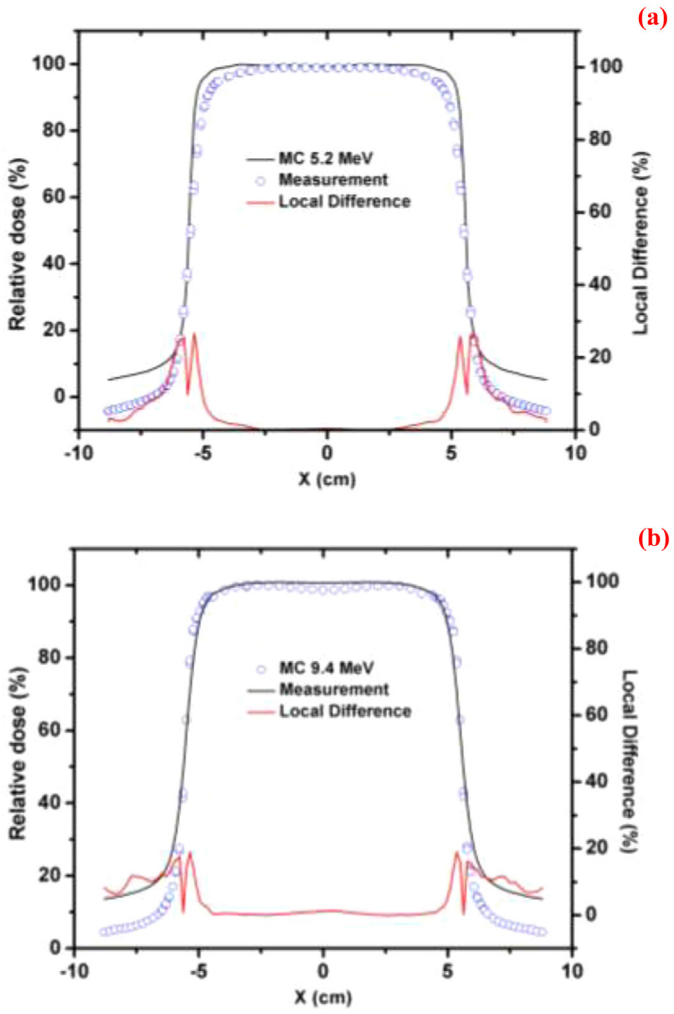

Fig. 7. Calculated and measured dose profiles for the (a) 6 MV and (b) 10 MV Elekta Infinity™ photon beam and the local dose difference between measurement and calculation.

incident electron energy, respectively. All the local differences are less than 2% for the descending part of the curves (Fig. 6(b)). The PDD results obtained from calculation and measurement show that the best agreement is obtained for a local dose difference of 9.4 MeV to simulate 10 MV photon beam.

3.2. Determination of linac geometry

Beam profiles were calculated in 10 cm (Fig. 7). The calculation results were validated with measurements. Statistical uncertainty of the calculated beam profiles was between 0.6% and 1.3% in the flat region of the profiles. For a better comparison between measurement and calculations, we considered three regions in our profiles including (1) the flat or umbra region, (2) the penumbra region, and (3) the low dose, out of field region.[38] For the flat region, the local differences were up to 2% for all field sizes and depths. For the second region, local differences of up to 10% were seen. In the low-dose region, which is located outside the geometric border of the field, local differences were up to 18%.

There are several recommendations for evaluating dose calculation model's performance in different situations, including simple homogenous geometry and complex geometry.[38,39] Venselaar et al. (2001) recommended different criteria for the acceptance of calculation results in the water phantom. Their proposed values of tolerances are as follows: (1) umbra region, 2%; (2) penumbra region, 10%; (3) outside beam edge, 30%.[38] For 6 MV photon beam, the average local dose difference was 4.14, 15.88, and 10.88%, in penumbra, umbra, and outside beam edge, respectively. On the other hand, the average local dose different in umbra, penumbra and outside beam edge were 0.67, 8.53, and 11.25%, respectively for 10 MV.

Table 1
Information about particles in scoring plane.

Energy (MV)	Scoring plane	Number of particles in phsp files		
		All particles	Photons	Electrons
6	Part 1	84522344	83583477	938867
	Part 2	85297377	84640902	656475
10	Part 1	68711530	67286103	1425427
	Part 2	73369353	72118784	1250569

Comparing local dose differences found in our results in the determination of incident electron energy and Linac geometry for $10 \times 10\,cm^2$ field size with their criteria shows that our MC model results are acceptable, and our model can be used for dose calculation in other situations and different field sizes. Electron energy used to simulate Linac Elekta Infinity™ 6 and 10 MV photon beam was 5.2 and 9.4 MeV, respectively based on the recommendation from Venselaar et al. (2001) although there were still significant differences in the penumbra area for 6 MV. The types and position settings of mlc leafs were varied and tested to obtain a smaller local difference in the penumbra region but this difference value does not change significantly in 6 MV energy. The electron energy obtained in this commissioning process was compared to another Varian linear accelerator with the same beam energy.[6,7] The electron energy of Varian Linac a has higher value than the Elekta in this study.

3.3. Particle information in scoring planes

The particle information stored in phsp files part 1 and 2 is shown in Table 1. The number of the electron in 6 MV photon beam was 1.11% and 0.77% of the total particles scoring plane for part 1 and part 2, respectively, and 2.07% and 1.70% for 10 MV photon beam. The number of electron contamination in phsp 1 is more than in phsp 2. Some electrons produced before mlc (scoring plane 1) caused this, blocked by mlc, and they did not reach scoring plane 2 in SSD 100 cm. In general, electrons are mixed at a large scattering angle (far from the beam axis) so that they were more likely to be blocked by mlc. On the other hand, the number of electron contamination increased for high energy Linac beam both on scoring plane 1 and 2. Contamination for 6 and 10 MV photon beam was larger than Varian accelerator with the same energy.[6,7] This was due to the difference of Linac geometry material. Varian linac's material generally consists of tungsten, which significantly contributes to electron contamination released from Linac and has an effect on the increasing dose in the surface area of the phantom.

The fluence distributions for the 6 and 10 MV $10 \times 10\,cm^2$ beams for scoring plane 1 and 2 in the X and Y direction as a function of the distance to the central beam axis are shown in Fig. 8. The MC calculation demonstrated that the particles fluence in phsp 1 was 10 times greater than in phsp 2 for all beam energy. The shape of the fluence curve on scoring plane 1 is strongly influenced by the shape of the flattening filter where the particle fluence in the central beam axis was less than at the edge of the radiation field. Particles from phsp 2 were collimated in the beam before entering mlc, JAWS, and scoring plane 2. As seen from this figure, the total fluence in scoring plane 2 remains relatively constant inside the field ($-5 < x < 5$ cm) and decreases sharply immediately after the geometric edge of the field ($x > 5$ cm). The Linac geometry was symmetric, so the X and Y fluence was identical.

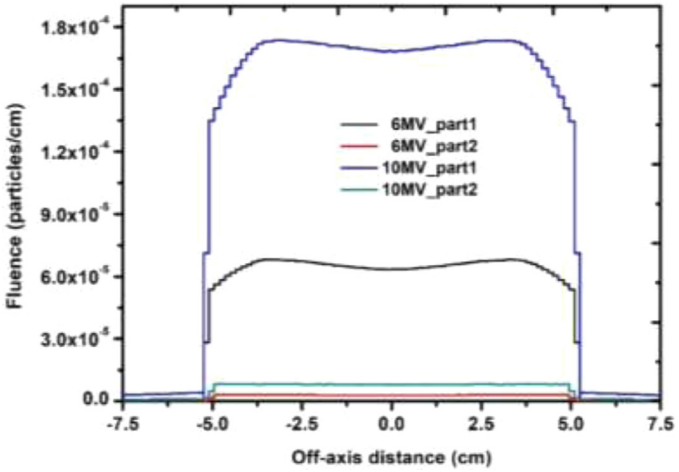

Fig. 8. Fluence distribution of particles in scoring plane 1 and 2 for 6 and 10 MV photon beam.

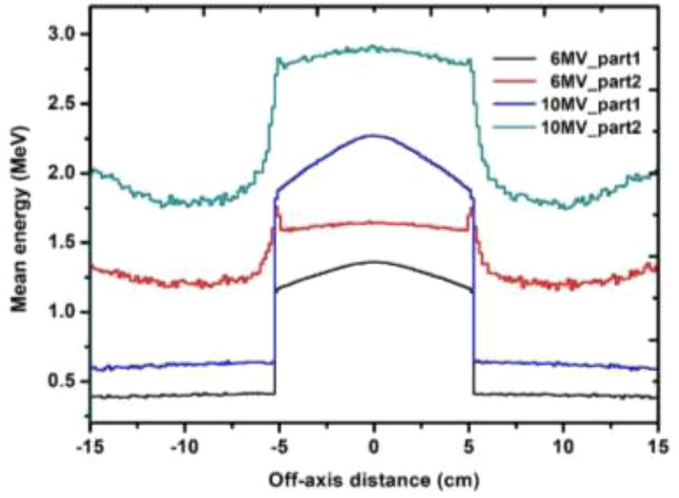

Fig. 9. Mean energy of particles in scoring plane 1 and 2 of 6 and 10 MV photon beam.

Fig. 9 illustrates the mean photon energy for these beams as a function of the distance from the beam central axis at the phantom surface. The field was divided into 602 rectangular bins, and the mean energy for each bin was calculated from -15 to 15 cm in the x-direction for phsp 1 and phsp 2. The mean energy of the particles in scoring plane 1 was different from scoring plane 2. For the 6 MV beams, the mean energy for the particles in phsp 1 was between 1.15 and 1.36 MeV while it was between 1.34 MeV and 1.76 MeV in scoring plane 2. For the 10 MV beams, it ranged from 1.88 MeV to 2.27 MeV and 1.78 MeV to 2.92 MeV in scoring plane 1 and 2, respectively. The mean energy in phsp 1 was relatively constant in the field (-5 to 5 cm), and the value decreased out of field in 6 and 10 MV. This mean energy was strongly related to the particle energy in the scoring plane. The out-of-field particles consist of electron contamination produced from interactions between photon and collimator. These particles will scatter with the large angle and have mean energy lower than the particles in the central beam axis.

The dominant particle interactions in linac head are photoelectric effect, Compton scattering, and pair production. Therefore, there is unwanted particle contamination such as electrons and positrons produced in Linac beside photons. In the Compton scattering, the scattering angle of a particle depends on its energy. The

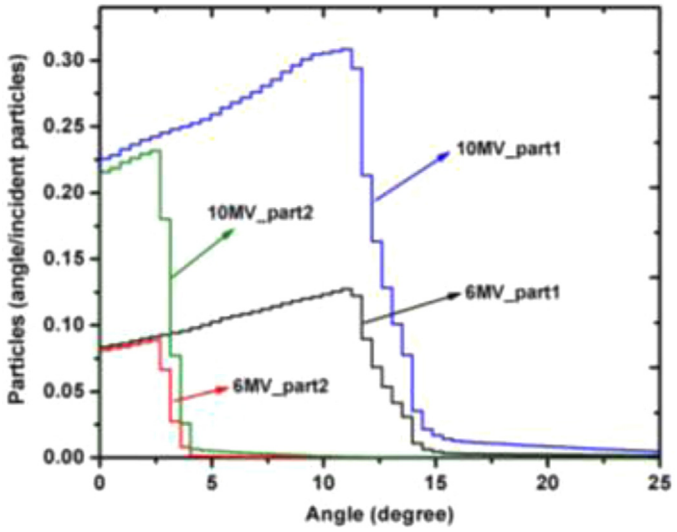

Fig. 10. Angular distribution of particles in scoring plane 1 and 2 of 6 and 10 MV photon beam.

Table 2
OFs deviation between MC simulation and semiflex/microDiamond detector.

Field size (cm^2)	Deviation (%)			
	Semiflex vs MC		microDiamond vs MC	
	6 MV	10 MV	6 MV	10 MV
2×2	3.55	5.29	2.73	1.42
3×3	1.80	3.75	1.47	0.35
5×5	1.19	1.79	1.02	0.15
6×6	0.72	1.30	0.47	0.08
8×8	1.82	1.79	1.6	0.15
10×10	0	0	0	0

low-energy particle will scatter within a large scattering angle and vice versa. Fig. 10 shows the angular distribution of particles in scoring plane 1 and 2 for 6 and 10 MV photon beam. The scattering angle of the particle in scoring plane 1 was between 0 – 15° and 0 – 25° for 6 and 10 MV, respectively. The scattering angle of the particles was reduced after the beam has been collimated (0 – 8° for 6 MV and 0 – 5° for 10 MV). The low-energy particles was reduced and blocked by the collimator.

In Fig. 11, the particle energy spectra in scoring plane 1 and 2 are presented for the 6 and 10 MV beam with a field size of $10 \times 10\ cm^2$ at the phantom surface. The energy spectra show a much-defined peak at around 0.49 MeV, and the peak value did not change in scoring plane 2 for 6 MV. The peak shifts to a higher energy for 10 MV photon beam (0.55 MeV). The collimation (mlc) only reduced the number of particles but did not change the photon energy produced in 6 and 10 MV photon beam Linac.

3.4. Output factors of 6 and 10 MV photon beam

The photon output factor is shown in Fig. 12 for square field sizes from 2 cm up to 10 cm obtained from measurements together with corresponding values from the MC calculation. The output factors from MC calculation ranged between 0.82 and 1.00 for 6 MV and 0.83 and 1.00 for 10 MV. The OFs from MC calculation was more significant than the semiflex and microDiamond measurement for both 6 and 10 MV photon beam.

The Eq. (4) was used to determine the relative deviation of OFs from measurement and MC calculation for specific field sizes (Table 2). The measured OFs using the different detectors are in good agreement with simulation within less than 2% for field

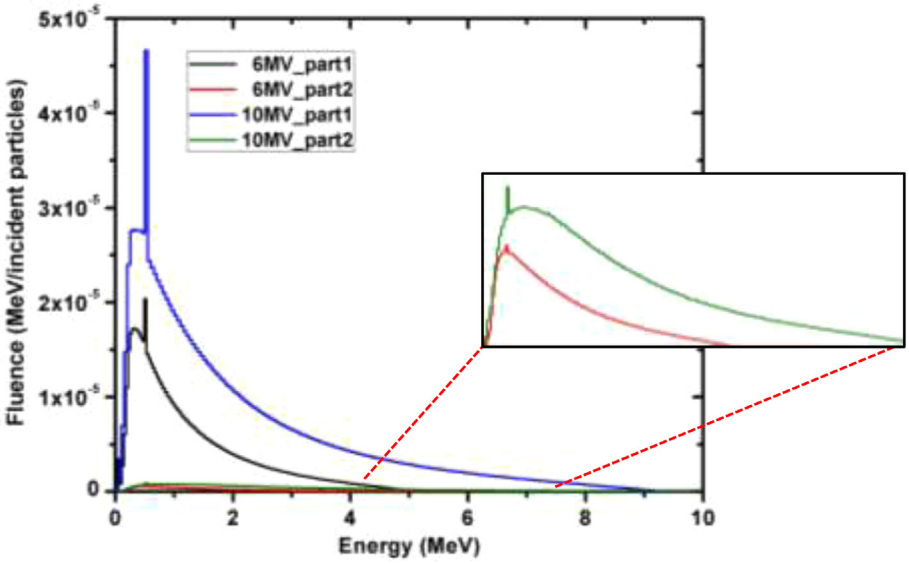

Fig. 11. Spectral distribution of particles in scoring plane 1 and 2 for the 6 and 10 MV photon beam.

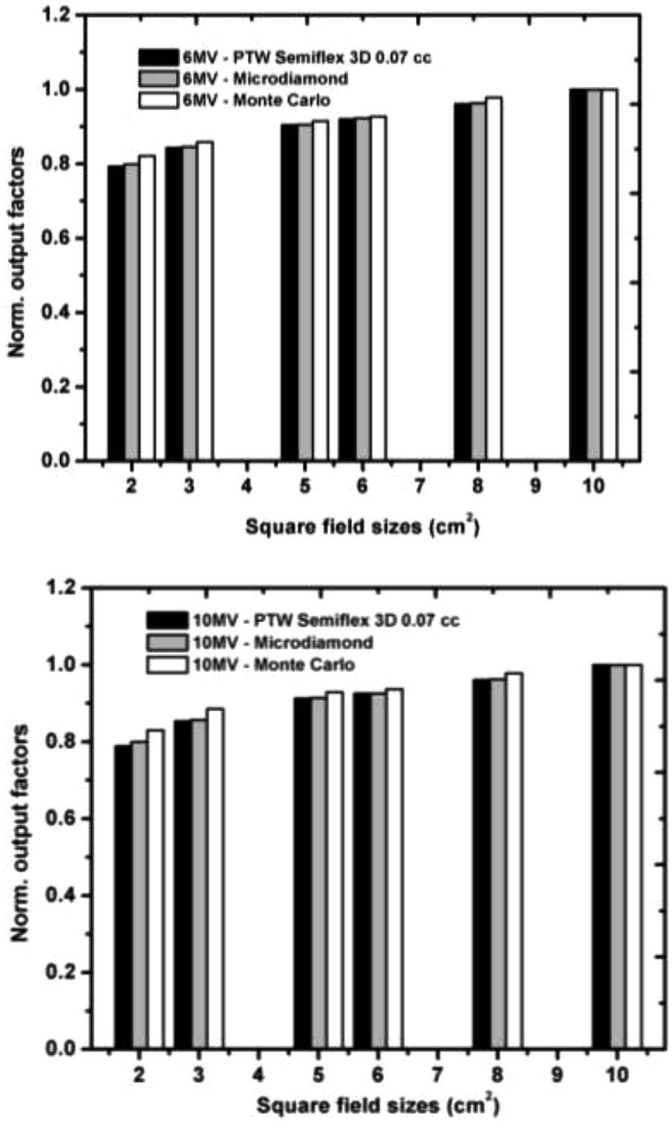

Fig. 12. Normalized OFs of 6 and 10 MV photon beam.

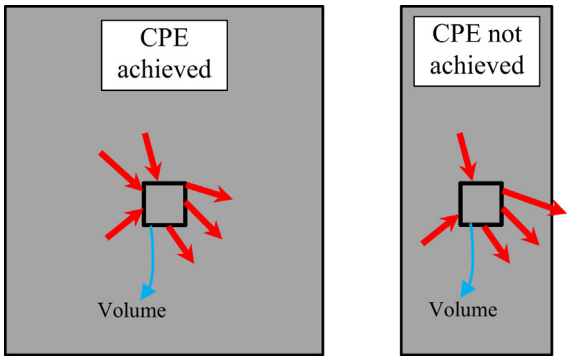

Fig. 13. Illustration of lateral charged particle equilibrium (CPE).

sizes $3 \times 3\ cm^2$ or larger for the considered energies. For the field size $2 \times 2\ cm^2$, the OFs deviation between semiflex detector and MC simulation for 10 MV beam show the most significant value among the other deviations. Between the MC simulation and the PTW semiflex ion chamber, the deviation goes up to 5.29%. The charged particle equilibrium (CPE) in high-energy Linacs for the small field (field size less than $5 \times 5\ cm^2$) will not be achieved because the radius of the beam was smaller than the maximum range of secondary charged particle. The illustration of achieved and non-achieved CPE is shown in Fig. 13.

The CPE exists in a scoring volume if energy carried in and out of a volume is equal. In a large field, there are electrons with a particular type and energy entering from another area to compensate the identically charged particles leaving the volume. This situation does not occur in small field sizes. The Bragg-Gray cavity theory assumption was ineffective in small field cases. In Monte Carlo simulation, this CPE was calculated in dose distribution to get accurate results. Therefore, the OFs from MC simulation have a slightly different value compared to measurement results. This phenomenon was seen in all field sizes and beam energy (Fig. 11). Haryanto et al. (2004) and Fukata et al. (2018) reported the same result as that measured for $2 \times 2\ cm^2$ field size has a significant deviation compared with measurement results.[18,40]

Krongkietlearts et al. (2016) calculated output factors for Varian Clinac iX6 MV beams using EGSnrc and found a different pattern. Their data were normalized to the $10 \times 10\ cm^2$ field. The OFs from microDiamond detector gives higher results than semiflex detector

and MC simulation with a deviation of less than 2% for field size 1×1, 2×2, 3×3, and $5 \times 5\,cm^2$. Other publications have reported the over responses of measurement using semiflex detector in the small field.[30]

4. Conclusion

Commissioning data of photon beam of energy 6 and 10 MV produced by Elekta Infinity™ platform installed in Radiotherapy Department at Concord International Hospital, Singapore were collected. The commissioning results indicated that the initial electron energy was 5.2 and 9.4 MeV to simulate 6 and 10 MV photon beam, respectively.

The most important result in this work comes from OFs resulted from MC calculation. This value was more significant than the OFs from measurement using semiflex and microDiamond for all beam energies and field sizes. This higher result is due to the CPE phenomenon calculated in Monte Carlo simulation, and it was not achieved during measurements of $2 \times 2\,cm^2$ field size.

Conflict of interest

None.

Financial disclosure

None.

Acknowledgment

Authors would like to thank Institute for Insentif In House Post Doctoral 2018, World Class University, Institut Teknologi Bandung, Indonesia.

References

1. Ding GX. Dose discrepancies between Monte Carlo calculations and measurements in the build-up region for a high-energy photon beam. *Med Phys*. 2002;29(11):2459–2463.
2. Fix MK, Keall PJ, Dawson K, Siebers JV. Monte Carlo source model for photon beam radiotherapy: Photon source characteristics. *Med Phys*. 2004;31(11):3106–3121.
3. Yarahmadi M, Nedaie HA, Allahverdi M, Asnaashari Kh, Sauer OA. Small photon field dosimetry using EBT2 Gafchromic film and Monte Carlo simulation. *International Journal of Radiation Research*. 2013;11(4):215–224.
4. Javedan K, Feygelman V, Zhang RR, et al. Monte Carlo comparison of superficial dose between flattening filter free and flattened beams. *Phys Med*. 2014;30(4):503–508.
5. Teke T, Duzenli C, Bergman A, Viel F, Atwal P, Gete E. Monte Carlo validation of the TrueBeam 10XFFF phase–space files for applications in lung SABR. *Med Phys*. 2015;42(12):6863–6874.
6. Yani S, Dirgayussa IGE, Rhani MF, Sog RCX, Haryanto F, Arif I. Monte Carlo study on electron contamination and output factors of small field dosimetry in 6 MV photon beam. *Smart Sci*. 2016;4(2):87–94.
7. Yani S, Rhani MF, Soh RCX, Haryanto F, Arif I. Monte Carlo simulation of varian clinac iX 10 MV photon beam for small field dosimetry. *Int J Radiat Res*. 2017;15(3):275–282.
8. Mohammed M, El Bardouni T, Chakir E, Boukhal H, Saeed M, Ahmed A-A. Monte Carlo simulation of Varian Linac for 6 MV photon beam with BEAMnrc code. *Radiat Phys Chem*. 2018;144:69–75.
9. Tartar A. Monte Carlo simulation approaches to dose distributions for 6 MV photon beams in clinical linear accelerator. *Biocybern Biomed Eng*. 2014;34:90–100.
10. Faria FP, Reynaldo S, Fonseca TCF, Lacerda MAS, Da Silva TA. Monte Carlo simulation applied to the characterization of an extrapolation chamber for beta radiation dosimetry. *Radiat Phys Chem*. 2015;116:226–230.
11. Yani S, Tursinah R, Rhani MF, Haryanto F, Arif I. Neutron contamination of Varian Clinac iX 10 MV photon beam using Monte Carlo simulation. *J Phys Conf Ser*. 2016;694:012020.
12. Hosseinzadeh E, Banaee N, Nedaie HA. Monte Carlo calculation of photoneutron dose produced by circular cones at 18 MV photon beams. *Rep Pract Oncol Radiother*. 2018;23:39–46.
13. Moskvin V, DesRosiers C, Papiez L, Timmerman R, Randall M, DesRosiers P. Monte Carlo simulation of the Leksell Gamma Knife: I. Source modelling and calculations in homogeneous media. *Phys Med Biol*. 2002;47(12):1995–2011.
14. Benmakhlouf H, Sempau J, Andreo P. Output correction factors for nine small field detectors in 6 MV radiation therapy photon beams: A PENELOPE Monte Carlo study. *Med Phys*. 2014;41(4):041711-1-12.
15. Sardari D, Maleki R, Samavat H, Esmaeeli A. Measurement of depth-dose of linear accelerator and simulation by use of Geant4 computer code. *Rep Pract Oncol Radiother*. 2010;15(3):64–68.
16. Bakkali JE, Bardouni TE, Zoubair M, Boukhal H. Validation of monte-carlo Geant4 code for saturne 43 LINAC. *International Journal of Innovation and Applied Studies*. 2013;4(2):424–436.
17. Seppala J, Voutilainen A, Heikkila J, Vauhkonen M. Surface doses of flattening filter fee beams with volumetric modulated arc delivery for breast cancer. *Phys Imaging Radiat Oncol*. 2017;2:17–22.
18. Haryanto F, Fippel M, Laub W, Dohm O, Nusslin F. Investigation of photon beam output factors for conformal radiation therapy—Monte Carlo simulations and measurements. *Phys Med Biol*. 2002;47:N133–N143.
19. Borges C, Zarza-Moreno M, Heath E, Teixeira N, Vaz P. Monte Carlo modeling and simulations of the High Definition (HD120) micro MLC and validation against measurements for a 6 MV beam. *Med Phys*. 2012;39(1):415–423.
20. Toutaoui A, Ait chikh S, Khelassi-Toutaoui N, Hattali B. Monte Carlo photon beam modeling and commissioning for radiotherapy dose calculation algorithm. *Phys Med*. 2014;30(7):833–837.
21. Mashud MAA, Tariquzzaman M, Alam MJ, Zakaria GA. Photon beam commissioning of an Elekta Synergy linear accelerator. *Polish J Med Phys Eng*. 2017;23(4):115–119.
22. Bakkali JE, Bardouni TE. Validation of Monte Carlo Geant4 code for a 6 MV varian linac. *J King Saud Univ - Sci*. 2017;29(1):106–113.
23. Scott AJD, Nahum AE, Fenwick JD. Using a Monte Carlo model to predict dosimetric properties of small radiotherapy photon fields. *Med Phys*. 2008;35(10):4671–4684.
24. Sheikh-Bagheri D, Rogers DWO. Monte Carlo calculation of nine megavoltage photon beam spectra using the BEAM code. *Med Phys*. 2002;29(3):391–402.
25. Verhaegen F, Mubata C, Pettingell J, et al. Monte Carlo calculation of output factors for circular, rectangular, and square fields of electron accelerators (6–20 MeV). *Med Phys*. 2001;28(6):938–949.
26. Das IJ, Ding GX, Ahnesjo A. Small fields: Nonequilibrium radiation dosimetry. *Med Phys*. 2008;35(1):206–215.
27. Fan J, Paskalev K, Wang L, et al. Determination of output factors for stereotactic radiosurgery beams. *Med Phys*. 2009;36(11):5292–5300.
28. Bassinet C, Huet C, Derreumaux S, et al. Small fields output factors measurements and correction factors determination for several detectors for a CyberKnife and linear accelerators equipped with microMLC and circular cones. *Med Phys*. 2013;40(7):071725-1-12.
29. Francescon P, Cora S, Cavedon C. Total scatter factors of small beams: A multidetector and Monte Carlo study. *Med Phys*. 2008;35(2):504–513.
30. Cheng JY, Ning H, Arora BC, Zhuge Y, Miller RW. Output factor comparison of Monte Carlo and measurement for Varian TrueBeam 6 MV and 10 MV flattening filter-free stereotactic radiosurgery system. *J Appl Clin Med Phys*. 2016;17(3):100–110.
31. Krongkietlearts K, Tangboonduangjit P, Paisangittisakul N. Determination of output factor for 6 MV small photon beam: Comparison between Monte Carlo simulation technique and microDiamond detector. *J Phys Conf Ser*. 2016;694:012019.
32. Godson HF, Ravikumar M, Ganesh KM, Sathiyan S, Ponmalar YR. Small field output factors: Comparison of measurements with various detectors and effects of detector orientation with primary jaw setting. *Radiat Meas*. 2016;85:99–110.
33. Gholampourkashi S, Cygler JE, Belec J, Vujicic M, Health E. Monte Carlo and analytic modeling of an Elekta Infinity linac with Agility MLC: Investigating the significance of accurate model parameters for small radiation fields. *J Appl Clin Med Phys*. 2019;20(1):55–67.
34. Rogers DWO, Walters B, Kawrakow I. *BEAMnrc users manual (Report PIRS-0509)*. Ottawa: National Research Council of Canada; 2015.
35. Walters B, Kawrakow I, Rogers DWO. *DOSXYZnrc users manual (Report PIRS-0794)*. Ottawa: National Research Council of Canada; 2015.
36. Konefał A, Bakoniak M, Orlef A, Maniakowski Z, Szewczuk M. Energy spectra in water for the 6 MV X-ray therapeutic beam generated by Clinac-2300 linac. *Radiat Meas*. 2015;72:12–22.
37. Cranmer-Sargison G, Wetson S, Evans JA, Sidhu NP, Thwaites DI. Implementing a newly proposed Monte Carlo based small field dosimetry formalism for a comprehensive set of diode detectors. *Med Phys*. 2011;38(12):6592–6602.
38. Venselaar J, Welleweerd H, Mijnheer B. Tolerances for the accuracy of photon beam dose calculations of treatment planning systems. *Radiother Oncol*. 2001;60(2):191–201.
39. Hartmann Siantar CL, Walling RS, Daly TP, et al. Description and dosimetric verification of the PEREGRINE Monte Carlo dose calculation system for photon beams incident on a water phantom. *Med Phys*. 2001;28(7):1322–1337.
40. Fukata K, Sugimoto S, Kurokawa C, Saito A, Inoue T, Sasai K. Output factor determination based on Monte Carlo simulation for small cone field in 10-MV photon beam. *Radiol Phys Technol*. 2018;11(2):192–201.